Candidate theory for the strange metal phase at a finite-energy window

Xiaochuan Wu,[1] Xiao Chen,[2] Chao-Ming Jian,[2,3] Yi-Zhuang You,[4] and Cenke Xu[1]
[1]*Department of Physics, University of California, Santa Barbara, California 93106, USA*
[2]*Kavli Institute of Theoretical Physics, Santa Barbara, California 93106, USA*
[3]*Station Q, Microsoft Research, Santa Barbara, California 93106-6105, USA*
[4]*Department of Physics, Harvard University, Cambridge, Massachusetts 02138, USA*

(Received 9 April 2018; revised manuscript received 11 September 2018; published 11 October 2018)

We propose a lattice model for strongly interacting electrons with the potential to explain the main phenomenology of the strange metal phase in the cuprate high-temperature superconductors. Our model is motivated by the recently developed "tetrahedron" rank-3 tensor model that mimics much of the physics of the better-known Sachdev-Ye-Kitaev (SYK) model. Our electron model has the following advantageous properties: (1) it needs only one orbital per site on the square lattice. (2) It does not require any quenched random interaction. (3) It has local interactions and respects all the symmetries of the system. (4) The soluble limit of this model has a longitudinal dc resistivity that scales linearly with temperature within a finite temperature window. (5) Again, the soluble limit of this model has a fermion pairing instability in the infrared, which can lead to either superconductivity or a "pseudogap" phase. The linear-T longitudinal resistivity and the pairing instability originate from the generic scaling feature of the SYK model and the tetrahedron tensor model.

DOI: 10.1103/PhysRevB.98.165117

I. INTRODUCTION

The non-Fermi-liquid (NFL) state represents a family of exotic metallic states that do not have long-lived quasiparticles and hence behave fundamentally differently from the standard Landau Fermi-liquid theory [1–11]. The NFLs usually occur at a certain quantum critical point in itinerant fermion systems, and the quantum critical fluctuations couple strongly with the fermions and hence "kill" the quasiparticles. But the most well known (yet poorly understood) NFL, the "strange metal" phase at the optimal doping of the cuprate high-temperature superconductors, seems more generic than the by-product of a certain quantum critical point because its anomalous temperature dependence of the longitudinal dc resistivity ($\rho \sim T$) persists up to a rather high temperature in the phase diagram [12–16], which is presumably much higher than the ultraviolet cutoff of any possible quantum critical point in the system. However, like many other NFLs [17–23], the strange metal phase is also preempted by a dome of "ordered phase" with a pair condensate of fermions (high-T_c superconductivity) at low temperature. Thus the strange metal phase is more fundamental than the superconductor phase itself: it is the "parent state" of the high-T_c superconductors, just like the Fermi liquid is the parent state (or normal state) of conventional BCS superconductors. And we better view this parent state as a generic non-Fermi-liquid state, instead of a quantum critical behavior.

A series of toy models for NFLs, despite their relatively unnatural forms, seems to capture the key universal features mentioned above. These models are the so-called Sachdev-Ye-Kitaev (SYK) model and its generalizations [24–31]. (1) The fermion Green's function in these models has a scaling behavior completely different from that of the noninteracting fermions in the infrared limit; thus it has no quasiparticle and by definition is a NFL. (2) It was found that the SYK model has marginally relevant "pairing instability" just like the ordinary Fermi-liquid state [32,33], which is again consistent with one of the universal features of the NFLs observed experimentally. (3) Recently measured charge density fluctuation of the strange metal [34] agrees with the unique scaling behavior of the SYK model [24]. (4) Last, but not least, recently, a generalization based on the SYK model has shown linear-T resistivity for a large temperature window, and the scaling behavior of the SYK model is the key for the linear-T resistivity [35] (a similar effect can be achieved in models with large-N generalization of the electron-phonon coupling [36–38]). All these developments suggest that some version of the SYK model and its generalizations may, indeed, be related to the strange metal phase the strange metal phase.

More often than not, an exactly soluble model has to sacrifice reality to some extent by making some artificial assumptions. To ensure its solubility, the original SYK model has the following necessary ingredients that make it unlikely to be directly related to the cuprates: (1) It needs an all-to-all four-fermion interaction, while a natural Hamiltonian for a real condensed-matter system usually has only local interactions. (2) The four-fermion interaction is fully random with a Gaussian distribution, which is also far from the real system. (3) So far the NFL models constructed based on generalizations of the SYK model all have a large number of fermion states on each unit cell of the lattice with a fully random all-to-all intra-unit-cell interaction [35,39–44], while the common wisdom is that the cuprate materials have only one active d orbital on each copper site.

In this work we will construct two lattice models for strongly interacting electrons that are still motivated by the

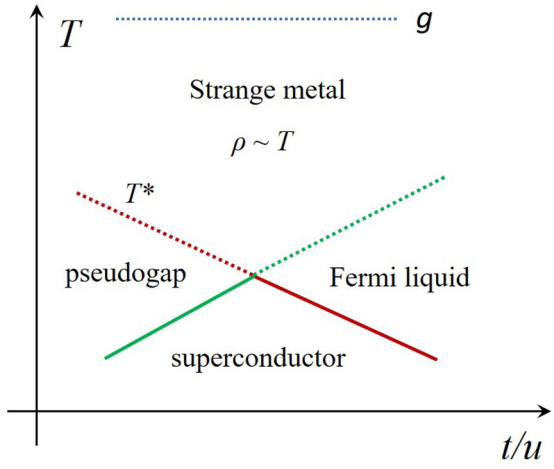

FIG. 1. The schematic phase diagram of our Hamiltonian (1) or (24) plus single-particle hopping parametrized by t and nearest-neighbor perturbation H_u [Eq. (19)] with coefficient u. The strange metal phase is dominated by only Eq. (1) or Eq. (24) and is characterized by the non-Fermi-liquid behavior and an anomalous linear-T scaling of the dc resistivity. The pseudogap crossover temperature scale T^* is given by Eq. (21). The exact phase boundaries need further calculations.

SYK physics but are much closer to real systems. (1) Our models need only one orbital per unit cell on the square lattice. (2) Our models have no quenched randomness. (3) Our models still capture the most desired physics of the SYK model, such as the linear-T scaling of the longitudinal dc resistivity and pairing instability in the infrared. In the soluble limit, the solution of our model is identical to the SYK model; thus our analytical results largely rely on the known solution of the SYK model in, for instance, Ref. [26]. But we will also check our analytical predictions based on the soluble limit by exact diagonalization of the minimal and most realistic version of our model away from the soluble limit in a finite system. The phase diagram of our proposed model for the physics near the strange metal phase including the low-energy phases induced by different perturbations considered in this paper is plotted in Fig. 1.

It was shown previously for the Sachdev-Ye model that away from the exactly soluble large-N limit [45], the SYK scaling still persists at a finite energy scale (for example, finite temperature), while instabilities due to $1/N$ corrections emerge at low energy which are suppressed (sub)exponentially with increasing N [46]. Although the exactly soluble version of our models still requires some large-N limit, by evaluating the next-order diagrams, we argue that for finite N, the scaling behavior of the large-N limit may still apply to an intermediate energy or temperature window, which is where the strange metal phase was observed in real systems.

II. THE HAMILTONIAN

Let us first write down the most important term of the interacting electron Hamiltonian that we will study on the square lattice:

$$H = \sum_j H_j,$$

$$H_j = U\hat{n}_j^2 + \sum_{\hat{e}=\hat{x},\hat{y}} J\left(\vec{S}_j \cdot \vec{S}_{j+\hat{e}} - \frac{1}{4}\hat{n}_j\hat{n}_{j+\hat{e}}\right) - K(\epsilon_{\alpha\beta}\epsilon_{\gamma\sigma}c^\dagger_{j,\alpha}c^\dagger_{j+\hat{x}+\hat{y},\beta}c_{j+\hat{y},\gamma}c_{j+\hat{x},\sigma} + \text{H.c.}), \quad (1)$$

where $\epsilon_{\alpha\beta}$ is a 2×2 antisymmetric matrix in spin space. Other terms, such as single-particle hopping, will later be treated as perturbations. We will study this model with a fixed particle density both analytically and numerically. Here $\hat{n}_j = \hat{n}_{j,\uparrow} + \hat{n}_{j,\downarrow}$ is the total electron number on site j, and $\vec{S}_j = \frac{1}{2}c^\dagger_j\vec{\sigma}c_j$ is the spin operator. Besides the standard charge density and spin interactions, we also turned on a "ring exchange" term with coefficient K, which takes a spin singlet pair of electrons on two diagonal sites of a plaquette to the two opposite diagonal sites of the same plaquette. This Hamiltonian preserves the square lattice symmetry (because this interaction has only even parity and spin singlet pairing between fermions) and also spin SU(2) symmetry.

We will try to make a connection between Eq. (1) and the SYK physics. As we explained previously, many necessary ingredients of the original SYK model are not very realistic. Instead of directly using the SYK model, our construction (1) is motivated by the randomness-free "tetrahedron" model (or the so-called rank-3 tensor model) [29,30,47]:

$$H_1^t = \frac{g}{(N_aN_bN_c)^{1/2}}c^\dagger_{a_1b_1c_1}c^\dagger_{a_2b_2c_1}c_{a_1b_2c_2}c_{a_2b_1c_2}. \quad (2)$$

Here $a_1, a_2 = 1\cdots N_a$, $b_1, b_2 = 1\cdots N_b$, and $c_1, c_2 = 1\cdots N_c$. This model has a $\mathrm{U}(N_a)\times\mathrm{U}(N_b)\times\mathrm{O}(N_c)$ symmetry. It was shown in the literature that, in the large-N_i limit, the dominant contribution to the Fermion Green's function comes from a series of "melon Feynman diagrams," which can be summed analytically by solving the Schwinger-Dyson equation.

To make a connection to electron systems, the first step is to modify the tetrahedron model as follows:

$$H_2^t = -\frac{g}{(N_aN_bN_c)^{1/2}} \times \mathcal{J}_{c_1,c_1'}\mathcal{J}_{c_2,c_2'}c^\dagger_{a_1b_1c_1}c^\dagger_{a_2b_2c_1'}c_{a_1b_2c_2}c_{a_2b_1c_2'}, \quad (3)$$

where $\mathcal{J}$ is the antisymmetric matrix associated with the $\mathrm{Sp}(N_c)$ group and $\mathcal{J}_{ab}c_ac_b$ forms an $\mathrm{Sp}(N_c)$ singlet. The total symmetry of this model is now $\mathrm{U}(N_a)\times\mathrm{U}(N_b)\times\mathrm{Sp}(N_c)$. The solubility of this model is unchanged from Eq. (2) in the large-N_i limit, and the single-particle Green's function in this limit is identical to the disorder-averaged Green's function of the SYK model [26]:

$$G(\tau) = -\mathcal{B}(\theta)e^{-2\pi T\mathcal{E}\tau}\sqrt{\frac{\pi T}{2g\sin(\pi T\tau)}}, \quad (4)$$

$$G(i\omega)_{T=0} = \frac{\mathcal{B}(\theta)}{\sin\left(\frac{\pi}{4}+\theta\right)}\frac{e^{-i\mathrm{sgn}[\omega]\left(\frac{\pi}{2}+\theta\right)}}{|2g\omega|^{\frac{1}{2}}}, \quad (5)$$

where a real angle parameter $-\frac{\pi}{4} < \theta < \frac{\pi}{4}$ and the spectral asymmetry $\mathcal{E}$ have been introduced. Both parameters depend on the charge density, and they are related to each other by

$$e^{2\pi\mathcal{E}} = \frac{\sin\left(\frac{\pi}{4}+\theta\right)}{\sin\left(\frac{\pi}{4}-\theta\right)}. \tag{6}$$

The angle $\theta = 0$ corresponds to the case of half filling. By solving consistent equations with the same method as Ref. [26], the coefficient $\mathcal{B}$ is found to be

$$\mathcal{B}(\theta) = \left(\frac{1}{\pi\cos(2\theta)}\right)^{\frac{1}{4}} \sin\left(\frac{\pi}{4}+\theta\right). \tag{7}$$

In Eq. (4), we have assumed $0 < \tau < \beta$ in the Green's function, and the Green's function with $-\beta < \tau < 0$ is determined by the standard relation $G(\tau+\beta) = -G(\tau)$.

Now we can draw a connection between the modified tetrahedron model (3) and our original model (1). When $U = K = \eta J/2$ ($\eta = \pm 1$), the total Hamiltonian (1) is equivalent to the following model with $N = 3$ and $M = 2$:

$$H = \sum_{j} \sum_{r,r'=-(N-1)/2}^{(N-1)/2} \sum_{\alpha,\beta,\gamma,\sigma=1}^{M} -\frac{g\eta_{r,r'}}{N\sqrt{M}} \times \mathcal{J}_{\alpha\beta}\mathcal{J}_{\gamma\sigma} c^{\dagger}_{j_x,j_y,\alpha} c^{\dagger}_{j_x+r,j_y+r',\beta} c_{j_x,j_y+r',\gamma} c_{j_x+r,j_y,\sigma}. \tag{8}$$

Just like the tetrahedron model (3), every fermion still carries three indices: the Sp(M) spin, the x coordinate, and the y coordinate. We will consider and numerically study two versions of the models with $\eta_{r,r'} = +1$ uniformly (when $N = 3$, $M = 2$, it corresponds to $U = K = -J/2$) and $\eta_{r,r'} = (-1)^{r+r'}$ (which corresponds to $U = K = +J/2$).

The minimal version of the model (8) with $N = 3$, $M = 2$ is identical to Eq. (1), which should be analogous to the case with $N_a = N_b = 3$ in Eq. (3). In analytical calculations, we always take the thermodynamics limit first (the sum of j is taken on a square lattice with infinite size). Then in the large-N and large-M limit, for both choices of $\eta_{r,r'}$, the fermion Green's function is still dominated by the "melon diagrams," and hence the Schwinger-Dyson equations, as well as their solutions, remain the same as models (2) and (3):

$$G_{j,j',\alpha,\beta}(\tau) = G(\tau)\delta_{j,j'}\delta_{\alpha,\beta}, \tag{9}$$

from which we can extract the fermion spectral function (local density of states)

$$\rho_f(\omega) = \sqrt{\frac{1}{gT}} \frac{\mathcal{B}(\theta)}{\sin\left(\frac{\pi}{4}+\theta\right)} \mathrm{Im}\left[\frac{ie^{-i\theta}}{2\pi} \frac{\Gamma\left(\frac{1}{4}+\frac{\beta(\omega-\omega_S)}{2\pi i}\right)}{\Gamma\left(\frac{3}{4}+\frac{\beta(\omega-\omega_S)}{2\pi i}\right)}\right]. \tag{10}$$

Here $\omega_S = 2\pi\mathcal{E}T$. The Fermion Green's function has the form of local quantum criticality, and the scaling dimension of the fermion operator is $\Delta[c] = 1/4$.

We have introduced a fixed fermion density, defined as

$$\mathcal{Q} = \frac{1}{M}\sum_{\alpha=1}^{M} \langle c^{\dagger}_{j,\alpha} c_{j,\alpha}\rangle. \tag{11}$$

The value of $\mathcal{Q}$ can be varied within the range $0 < \mathcal{Q} < 1$. Using the same method as Ref. [26], the relation between fermion density $\mathcal{Q}$ and the angle parameter θ in the Green's function is found to be

$$\mathcal{Q} = \frac{1}{2} - \frac{\theta}{\pi} - \frac{\sin(2\theta)}{4}, \quad -\frac{\pi}{4} < \theta < \frac{\pi}{4}. \tag{12}$$

The fact that the fermion Green's function (9) remains localized in space is due to the fact that the Hamiltonians (1) and (8) preserve the center of mass of the electrons on the square lattice. Any nonzero fermion correlation with a finite spatial separation would violate the center-of-mass conservation; thus the fermion Green's function is fully localized in space. Single-particle hopping will later be introduced as a perturbation, which breaks center-of-mass conservation and leads to spatial correlation between fermions and also charge transport.

For finite N and M, we need to estimate the corrections coming from the subdominant Feynman diagrams. For any diagram, if we evaluate it with the solution in the large-(N, M) limit, it will roughly lead to a "marginal" correction; namely, it will correct the large-(N, M) solution with a logarithmic function of infrared cutoff, say, the temperature. This is because in the large-(N, M) soluble limit the coupling constant g becomes marginal since the scaling dimension of the fermion operator is 1/4. Subdominant Feynman diagrams of SYK-like models were carefully calculated in Ref. [48], and the result is consistent with our expectation. Thus we expect that any subdominant diagram will, *at most,* lead to corrections with the form $\sim 1/N^A 1/M^B [\ln(\Lambda/T)]^C$, where A, B, and C are all positive numbers. This diagram will hence become significant only when

$$T \leqslant \Lambda \exp\left(-cN^{\frac{A}{C}} M^{\frac{B}{C}}\right), \tag{13}$$

where Λ is the ultraviolet cutoff of the system, which can be identified as g in our model. Thus we expect the correction to the NFL solution to be suppressed rapidly with increasing N and M; hence it is possible that there is a finite-energy window where the solution (9) applies. This is consistent with the expectation for the original Sachdev-Ye model away from the exactly soluble limit [46]. Away from the exactly soluble limit, the ground state has no finite entropy density.

III. PROPERTIES OF THE NFL

A. Longitudinal conductivity

Assuming Eq. (9) applies to a finite-energy window, we can use it to compute quantities at finite temperature within such an energy window. Because Eq. (1) conserves the center of mass of the electrons, it is incapable of transporting electric charge. More formally, this interaction term does not couple to the zero-momentum component of the external electromagnetic field, analogous to models studied previously with center-of-mass conservation [49,50]. Thus the single-particle hopping term is still responsible for charge transport. In cuprates both the nearest-neighbor and second-neighbor hoppings are important [51]. In the soluble large-(N, M) limit, we formally generalize the electric current density to the

following form:

$$J_x = \frac{1}{\sqrt{NM}}\left(\sum_\alpha itc^\dagger_{j,\alpha}c_{j+\hat{x},\alpha} + \sqrt{\frac{N-1}{2}}itc^\dagger_{j,\alpha}c_{j+\hat{x}\pm\hat{y},\alpha}\right) + \text{H.c.} \quad (14)$$

This electric current density can be derived by designing a corresponding single-electron hopping term in the large-(N, M) limit (which involves both nearest- and second-neighbor hopping) and coupling it to the external electromagnetic field.

Assuming the solution in the large-(N, M) limit (9) applies to a finite-energy window of the system, then according to the Kubo formula, the central task is to calculate the retarded current-current correlation function. The imaginary-time correlation function is defined as $C(J, J; \tau) = \langle \mathbb{T}_\tau J(\tau)J(0)\rangle$. We find the $\langle J_x\ J_y\rangle$ correlation vanishes due to the symmetry of the model, and the leading order nonzero contribution to $\langle J_x\ J_x\rangle$ takes the form $C(J, J; \tau) = -2t^2G(\tau)G(-\tau)$. Then we Fourier transform $C(J, J; \tau)$ to obtain the correlation function in the Matsubara frequency space:

$$C(J, J; i\omega_n) = 2t^2\int_\delta^{\beta-\delta} d\tau e^{i\omega_n\tau}G(\tau)G(\beta-\tau), \quad (15)$$

where we have regulated the integral by introducing a small positive cutoff δ. After removing the divergent term $\ln\delta$ (which does not contribute to the real part of the conductivity), we obtain the analytically continued correlation function

$$C(J, J; z) = -2\frac{t^2}{g}\mathcal{B}^2e^{-2\pi\mathcal{E}}\psi\left(\frac{1}{2} + \frac{\beta z}{2\pi i}\right), \quad (16)$$

where $\psi(z) = \frac{d}{dz}\ln\Gamma(z)$ is the polygamma function and the complex frequency z satisfies $\text{Im}z > 0$. The function $C(J, J; i\omega_n)$ can be obtained by setting $z \to i\omega_n$ in the above expression, and the retarded/advanced correlation function $C^{R/A}(J, J; \omega)$ is obtained by taking $z \to \omega \pm i0^+$. Finally, using the relation $\sigma(\omega) = \frac{1}{i\omega}C^R(J, J; \omega)$, we find the real part of the optical conductivity:

$$\text{Re}\sigma(\omega) = \frac{\sqrt{\pi}t^2}{4gT}\Upsilon_\sigma(\mathcal{Q}, \omega/T), \quad (17)$$

where

$$\Upsilon_\sigma(\mathcal{Q}, \omega/T) = \sqrt{\cos[2\theta(\mathcal{Q}]}\frac{\tanh(\omega/2T)}{\omega/2T} \quad (18)$$

is the scaling function of the conductivity. From another perspective, Υ_σ can also be computed from the convolution of the scaling function of the fermion spectral function ρ_f in Eq. (10).

By our definition, Υ_σ depends on both the fermion density $\mathcal{Q}$ and the ratio ω/T. The $\mathcal{Q}$ dependence of the conductivity is contained in the coefficient $\sqrt{\cos(2\theta)}$ in the scaling function $\Upsilon_\sigma(\mathcal{Q}, \omega/T)$, and the function $\theta(\mathcal{Q})$ can be obtained by inverting Eq. (12). The half filling $\theta = 0$ gives the maximum conductivity, as one would naively expect. Once we fix the ratio ω/T (for example, the dc limit with $\omega/T = 0$), the longitudinal conductivity $\sigma(\omega, T)$ is proportional to $1/T$, which is the most important phenomenon of the strange metal phase.

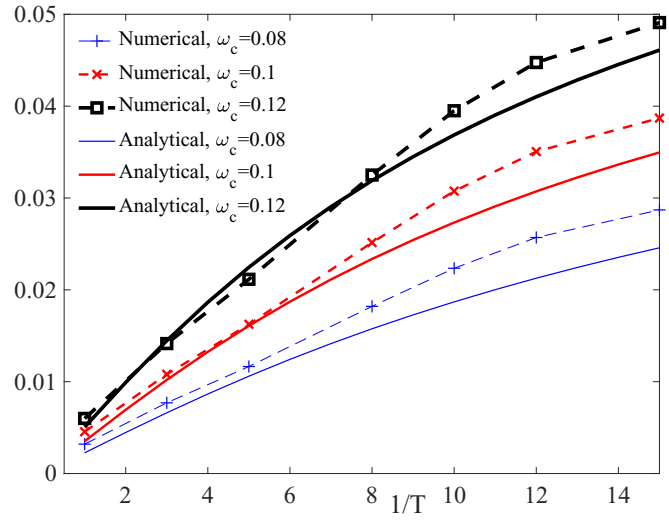

FIG. 2. The quantity $F(\omega_c, T) = \int_0^\infty d\omega e^{-\omega/\omega_c}\omega\sigma(\omega, T)$ extracted from exact diagonalization of Eq. (8) on a 3×4 lattice, with $g = 1$, $M = 2$, $N = 3$, and a fixed particle number $N_p = 4$. The solid lines are the plot of the same quantity calculated based on the scaling function (17). In the definition of electric current we have also taken $N = 3$, $M = 2$; namely, both the nearest-neighbor and second-neighbor hopping will contribute to conductivity. In this small system our data with a uniform $\eta_{r,r'} = +1$ compare better with the analytical solution in the large-(N, M) limit.

In the calculation above we have assumed that the correlation function between current operators factorizes into a product of two fermion Green's functions. This is true in the large-(N, M) limit using the current operator (14), and expression (17) is exact in this limit.

We also studied the minimal and most realistic version of our model, Eq. (1), with exact diagonalization on a small 3×4 lattice with periodic boundary conditions and a fixed particle number $N_p = 4$. With our numerical method, it is most convenient to compare the quantity $F(\omega_c, T) = \int_0^\infty d\omega e^{-\omega/\omega_c}\omega\sigma(\omega, T)$ with the analytical result (17). We found that the case with the uniform choice $\eta_{r,r'} = +1$ compares better with the solution in the large-(N, M) limit. The general shape of the function $F(\omega_c, T)$ obtained numerically is similar to the analytical expression in the large-(N, M) limit (Fig. 2), but further numerical evidence is demanded for larger system sizes for both choices of $\eta_{r,r'}$.

The value of the dc conductivity is tunable by the parameter t in the definition of the electric current (which is determined by the size of the hopping term) and the overall energy scale g. Thus the resistivity in the minimal version of our model can easily exceed the Mott-Ioffe-Regel limit; that is, it can naturally become the so-called bad metal, which is another puzzling phenomenon observed in cuprate materials and has attracted a lot of attention [52–54].

B. Pairing instability and pseudogap

Besides hopping, we can also turn on other perturbations in Eq. (1). For example, we can turn on the following

perturbation on every link of the lattice:

$$H_u = \sum_{\langle i,j\rangle} -\frac{u}{2M}(\Delta^\dagger_{i,j}\Delta_{i,j} + \Delta_{i,j}\Delta^\dagger_{i,j}). \tag{19}$$

Here $\Delta_{i,j} = \mathcal{J}_{\alpha\beta}c_{i,\alpha}c_{j,\beta}$ is a Sp(M) singlet pairing operator on a nearest-neighbor link $\langle i, j\rangle$. This term can be reorganized into a nearest-neighbor density-density interaction and a Heisenberg interaction using the Fierz identity of the symplectic Lie algebra [55].

This interaction term is marginal at the large-(N, M) limit because of power counting, again based on the fact that the fermion operator has a scaling dimension of 1/4, and in the large-(N, M) limit all of the renormalization from Eq. (8) to this term is contained in the renormalization of the fermion operator. In this limit, the renormalization group (RG) equation of u can be computed through the standard loop diagram in the same way as in Ref. [32], using the fermion Green's function in Eq. (5):

$$\frac{du}{d\ln l} = \frac{u^2}{\sqrt{g^2\pi\cos(2\theta)}}. \tag{20}$$

Thus the u term is marginally relevant in this limit, and it will likely lead to the fermion pairing instability just like the BCS instability of the ordinary Fermi liquid.

H_u and single-particle hopping will compete with each other under RG. H_u will become nonperturbative at scales T^*:

$$T^* \sim g\exp\left(-\sqrt{\pi\cos(2\theta)}\frac{g}{u}\right). \tag{21}$$

Assuming the single-particle hopping becomes nonperturbative at the scale E_0 (by naive power counting a single-particle hopping is indeed relevant and will become nonperturbative at the scale $E_0 \sim t^2/g$), then, obviously, there are two possible scenarios: If $E_0 > T^*$, the hopping term will dominate the low-energy physics and generate a Fermi sea. And at low energy the RG flow of u will be controlled by the standard RG equation of interactions on the Fermi sea, and again, u will be marginally relevant and lead to a pairing instability [56]. H_u and the band structure together will likely favor a d-wave superconductor [57–59] on the square lattice near half filling.

The possibility of $T^* > E_0$, i.e., u becoming nonperturbative first under renormalization while energy is decreased, is even more interesting. Without single-electron hopping, based on the RG equation (20) alone, one cannot determine the pairing symmetry. In fact, in this case, with decreasing temperature (energy scale), before forming a superconductor with global phase coherence, the system would favor forming Sp(M) spin-singlet fermion pairings on as many nearest-neighbor links as possible. At half filling, a generalization of Rokhsar's theorem [60] can be straightforwardly applied to our case, and the ground states of Eq. (19) in the large-M limit are all the "dimerized" configurations with one quarter of the links occupied by $M/2$ pairs of fermions that each form a Sp(M) singlet [61]. All these dimerized configurations are degenerate in the large-M limit [60]. Weak disorder and $1/M$ correction could energetically select a certain pattern of dimerization from the extensively degenerate configurations, as was observed experimentally [62]. This state has a single-particle excitation gap which necessarily breaks a Sp(M) singlet on one of the links, but there is no global fermion-pair phase coherence. This case could be identified as the pseudogap phase in the cuprate phase diagram above the superconducting dome.

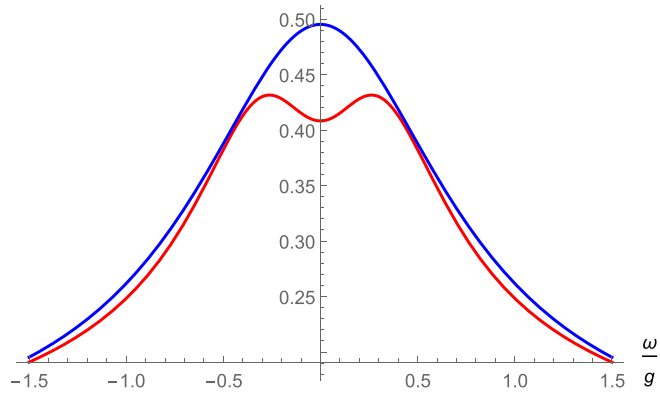

FIG. 3. The local density of states at half filling ($\theta = 0$) with $T > T^*$ and $\langle\Delta_{ij}\rangle = 0$ (top blue curve) and $T < T^*$ with nonzero $\langle\Delta_{ij}\rangle$ (bottom red curve). In the former case we have chosen $g\beta = 2$; in the latter case we have chosen $g\beta = 4.5$ and $(u\Delta)/(gM) = 0.15$ for illustration.

The "pseudogap" crossover temperature T^* is given by Eq. (21), below which the system develops a nonzero expectation value of $\langle\Delta_{ij}\rangle = \Delta$ on a maximal possible number of links based on our physical picture given above. With a nonzero Δ, for each pair of sites i and j coupled by the Sp(M) singlet pair, we consider the perturbation $\frac{u}{M}\Delta^*(\mathcal{J}_{\gamma\delta}c_{i,\gamma}c_{j,\delta}) +$ H.c. to the original model (3). Let us consider two sites ($j = 1, 2$) connected by a dimer. We introduce a $2M$-component fermion basis $\Psi = (c_{1,\alpha}\ ,\ c^\dagger_{2,\alpha})^T$ and the $2M \times 2M$ Green's function matrix $\mathcal{G}(\tau) \equiv -\langle\mathbb{T}_\tau\Psi(\tau)\Psi(0)^\dagger\rangle$. To the first order of Δ, the Green's function in the imaginary-frequency domain is given by

$$\mathcal{G}^{-1}(i\omega_n) = \begin{bmatrix} G^{-1}(i\omega_n) & \frac{u}{M}\Delta\mathcal{J} \\ \frac{u}{M}\Delta^*\mathcal{J}^{\mathrm{T}} & -G^{-1}(-i\omega_n) \end{bmatrix}, \tag{22}$$

where $G(i\omega_n)$ is the original single-fermion Green's function given by Eqs. (5) and (4). By inverting Eq. (22), we obtain the final Green's function $-\langle\mathbb{T}_\tau c_{1,\alpha}(\tau)c^\dagger_{1,\beta}(0)\rangle$:

$$\frac{\delta_{\alpha\beta}}{G^{-1}(i\omega_n) + \frac{u^2}{M^2}|\Delta|^2 G(-i\omega_n)}. \tag{23}$$

We can analytically continue this expression to real frequency to obtain the retarded Green's function on each site, whose imaginary part can be identified as the local density of states (see Fig. 3), where a pseudogap is manifest. In this calculation the Green's function depends on only the amplitude of $\langle\Delta_{ij}\rangle$; thus even if the phase angle of $\langle\Delta_{ij}\rangle$ is disordered, the pseudogap in the local density of states is still expected to exist.

A schematic global phase diagram with the parent strange metal phase dominated by H_s and the competition between perturbations H_u and single-particle hopping parametrized by t are depicted in Fig. 1.

We must stress that all the analysis discussed in this section is based on the physics of the tetrahedron model in the soluble

limit, which is identical to the disorder-averaged physics of the SYK model. No matter how exactly the SYK physics is realized in the real system, this analysis always applies. Our Eqs. (1) and (8) give only one possible realization of this physics. Very similar physics can be realized in another model discussed in the following section.

IV. ANOTHER POSSIBLE MODEL

Another model which is slightly less natural but probably leads to very similar physics is also worth discussion. Again, the most important term (but not the only term) of the Hamiltonian reads

$$H = \sum_j H_j,$$

$$H_j = U\hat{n}_j^2 + \sum_{\hat{e}=\hat{e}_1,\hat{e}_2} J\left(\vec{S}_j \cdot \vec{S}_{j+\hat{e}} - \frac{1}{4}\hat{n}_j\hat{n}_{j+\hat{e}}\right) - K(\epsilon_{\alpha\beta}\epsilon_{\gamma\sigma}c^\dagger_{j,\alpha}c^\dagger_{j+\hat{e}_1+\hat{e}_2,\beta}c_{j+\hat{e}_2,\gamma}c_{j+\hat{e}_1,\sigma} + \text{H.c.}), \quad (24)$$

where $\hat{e}_1 = \hat{x} + \hat{y}$ and $\hat{e}_2 = \hat{x} - \hat{y}$. This term has no interaction between sublattices A and B yet, and like before, we will consider the single-particle hoppings and interactions that mix the two sublattices as perturbations.

The advantage of this model is that we no longer need a large-N generalization of the hopping term. The ordinary nearest-neighbor hopping bridges the two sublattices; that is, it bridges two "SYK clusters" similar to the previously studied coupled SYK cluster models [63,64]. The nearest-neighbor hopping with coefficient t is a relevant perturbation based on the scaling dimension of the fermion operator $\Delta[c_j] = 1/4$ in the soluble limit. The scaling dimension of t is $\Delta[t] = 1/2$. Thus with the perturbation of the nearest-neighbor hopping, we expect the large-(N, M) solution of the tetrahedron model to be applicable roughly to the energy window $(t^2/g,\ g)$, and within this window the longitudinal conductivity $\sigma(\omega, T)$ takes the same form as the previous case. Other analysis like the perturbation of H_u [Eq. (19)] and pairing instability remains unchanged compared with the last model we considered.

V. SUMMARY AND DISCUSSION

In this work we proposed two strongly interacting electron models on the square lattice, with one orbital per unit cell. And we demonstrated that in a certain limit these models mimic the behavior of the "tetrahedron" tensor model and hence can be solved. The physics in this limit is consistent with the main phenomenology of the strange metal non-Fermi-liquid phase observed in the cuprates. We argue that away from this exactly soluble limit, there is still a finite-energy window where the solution is applicable. We then checked our predictions numerically by exactly diagonalizing the minimal version of the proposed Hamiltonian (which is away from the soluble limit and hence takes a realistic form) on a small lattice. We also discussed effects of perturbations, including the single-particle hopping, and argued that depending on the competition between two perturbations, the system can develop either a d-wave superconductor or a pseudogap phase at low temperature.

More numerical effort is demanded in the future to further analyze both our models, Eqs. (1) and (24). Also, more predictions on thermodynamics and transport can be made below the crossover temperature T^* where the system enters the pseudogap phase driven by H_u. The exact phase boundaries in the phase diagram (Fig. 1) also need further detailed calculations. In this work we have treated single-particle hopping as a perturbation on top of the SYK-like physics. A complete treatment of the interaction term [Eqs. (1) and (24)] together with single-particle hopping is demanded in the future in order to study the momentum space structure of our theory. We will leave these open questions to future studies.

ACKNOWLEDGMENTS

X.C. is supported by a postdoctoral fellowship from the Gordon and Betty Moore Foundation, under the EPiQS initiative, Grant No. GBMF4304, at the Kavli Institute for Theoretical Physics. C.X. is supported by the David and Lucile Packard Foundation and NSF Grant No. DMR-1151208. We acknowledge support from the Center for Scientific Computing from the CNSI, MRL, an NSF MRSEC (Grant No. DMR1121053). We also thank L. Balents, M. P. A. Fisher, S. A. Kivelson, S. Sachdev, and T. Senthil for very helpful discussions.

[1] H. V. Löhneysen, A. Rosch, M. Vojta, and P. Wölfle, Rev. Mod. Phys. **79**, 1015 (2007).
[2] J. Polchinski, Nucl. Phys. B **422**, 617 (1994).
[3] C. Nayak and F. Wilczek, Nucl. Phys. B **417**, 359 (1994).
[4] C. Nayak and F. Wilczek, Nucl. Phys. B **430**, 534 (1994).
[5] V. Oganesyan, S. A. Kivelson, and E. Fradkin, Phys. Rev. B **64**, 195109 (2001).
[6] S.-S. Lee, Phys. Rev. B **80**, 165102 (2009).
[7] D. F. Mross, J. McGreevy, H. Liu, and T. Senthil, Phys. Rev. B **82**, 045121 (2010).
[8] M. A. Metlitski and S. Sachdev, Phys. Rev. B **82**, 075127 (2010).
[9] M. A. Metlitski and S. Sachdev, Phys. Rev. B **82**, 075128 (2010).
[10] A. Schlief, P. Lunts, and S.-S. Lee, Phys. Rev. X **7**, 021010 (2017).
[11] Y. Schattner, S. Lederer, S. A. Kivelson, and E. Berg, Phys. Rev. X **6**, 031028 (2016).
[12] M. Gurvitch and A. T. Fiory, Phys. Rev. Lett. **59**, 1337 (1987).
[13] S. W. Tozer, A. W. Kleinsasser, T. Penney, D. Kaiser, and F. Holtzberg, Phys. Rev. Lett. **59**, 1768 (1987).
[14] S. Martin, A. T. Fiory, R. M. Fleming, L. F. Schneemeyer, and J. V. Waszczak, Phys. Rev. Lett. **60**, 2194 (1988).
[15] S. Martin, A. T. Fiory, R. M. Fleming, L. F. Schneemeyer, and J. V. Waszczak, Phys. Rev. B **41**, 846 (1990).
[16] C. M. Varma, P. B. Littlewood, S. Schmitt-Rink, E. Abrahams, and A. E. Ruckenstein, Phys. Rev. Lett. **63**, 1996 (1989).

[17] M. A. Metlitski, D. F. Mross, S. Sachdev, and T. Senthil, Phys. Rev. B **91**, 115111 (2015).
[18] Y. Wang and A. V. Chubukov, Phys. Rev. B **92**, 125108 (2015).
[19] I. Mandal, Phys. Rev. B **94**, 115138 (2016).
[20] S. Lederer, Y. Schattner, E. Berg, and S. A. Kivelson, Phys. Rev. Lett. **114**, 097001 (2015).
[21] Y. Wang, A. Abanov, B. L. Altshuler, E. A. Yuzbashyan, and A. V. Chubukov, Phys. Rev. Lett. **117**, 157001 (2016).
[22] S. Lederer, Y. Schattner, E. Berg, and S. A. Kivelson, Proc. Natl. Acad. Sci. USA **114**, 4905 (2017).
[23] E. Fradkin, S. A. Kivelson, and J. M. Tranquada, Rev. Mod. Phys. **87**, 457 (2015).
[24] S. Sachdev and J. Ye, Phys. Rev. Lett. **70**, 3339 (1993).
[25] A. Kitaev (unpublished).
[26] S. Sachdev, Phys. Rev. X **5**, 041025 (2015).
[27] J. Polchinski and V. Rosenhaus, J. High Energy Phys. 04 (2016) 001.
[28] J. Maldacena and D. Stanford, Phys. Rev. D **94**, 106002 (2016).
[29] E. Witten, arXiv:1610.09758.
[30] I. R. Klebanov and G. Tarnopolsky, Phys. Rev. D **95**, 046004 (2017).
[31] D. J. Gross and V. Rosenhaus, J. High Energy Phys. 02 (2017) 093.
[32] Z. Bi, C.-M. Jian, Y.-Z. You, K. A. Pawlak, and C. Xu, Phys. Rev. B **95**, 205105 (2017).
[33] Z. Luo, Y.-Z. You, J. Li, C.-M. Jian, D. Lu, C. Xu, B. Zeng, and R. Laflamme, arXiv:1712.06458.
[34] M. Mitrano, A. A. Husain, S. Vig, A. Kogar, M. S. Rak, S. I. Rubeck, J. Schmalian, B. Uchoa, J. Schneeloch, R. Zhong *et al.*, Proc. Natl. Acad. Sci. USA **115**, 5392 (2018).
[35] X.-Y. Song, C.-M. Jian, and L. Balents, Phys. Rev. Lett. **119**, 216601 (2017).
[36] Y. Werman, S. A. Kivelson, and E. Berg, npj Quantum Mater. **2**, 7 (2017).
[37] Y. Werman and E. Berg, Phys. Rev. B **93**, 075109 (2016).
[38] Y. Werman, S. A. Kivelson, and E. Berg, arXiv:1705.07895.
[39] Y. Gu, X.-L. Qi, and D. Stanford, J. High Energy Phys. 05 (2017) 125.
[40] R. A. Davison, W. Fu, A. Georges, Y. Gu, K. Jensen, and S. Sachdev, Phys. Rev. B **95**, 155131 (2017).
[41] S.-K. Jian and H. Yao, Phys. Rev. Lett. **119**, 206602 (2017).
[42] C.-M. Jian, Z. Bi, and C. Xu, Phys. Rev. B **96**, 115122 (2017).
[43] A. A. Patel, J. McGreevy, D. P. Arovas, and S. Sachdev, Phys. Rev. X **8**, 021049 (2018).
[44] D. Chowdhury, Y. Werman, E. Berg, and T. Senthil, Phys. Rev. X **8**, 031024 (2018).
[45] Actually, the original Sachdev-Ye model requires two parameters, N and M, be taken as infinite. Here for simplicity we use large-N to represent both limits.
[46] A. Georges, O. Parcollet, and S. Sachdev, Phys. Rev. B **63**, 134406 (2001).
[47] R. Gurau, Commun. Math. Phys. **304**, 69 (2011).
[48] S. Dartois, H. Erbin, and S. Mondal, arXiv:1706.00412.
[49] A. Paramekanti, L. Balents, and M. P. A. Fisher, Phys. Rev. B **66**, 054526 (2002).
[50] L. Balents and A. Paramekanti, Phys. Rev. B **67**, 134427 (2003).
[51] R. S. Markiewicz, S. Sahrakorpi, M. Lindroos, H. Lin, and A. Bansil, Phys. Rev. B **72**, 054519 (2005).
[52] N. E. Hussey, K. Takenaka, and H. Takagi, Philos. Mag. **84**, 2847 (2004).
[53] H. Takagi, B. Batlogg, H. L. Kao, J. Kwo, R. J. Cava, J. J. Krajewski, and W. F. Peck, Phys. Rev. Lett. **69**, 2975 (1992).
[54] V. J. Emery and S. A. Kivelson, Phys. Rev. Lett. **74**, 3253 (1995).
[55] S. Sachdev and N. Read, Int. J. Mod. Phys. B **05**, 219 (1991).
[56] R. Shankar, Rev. Mod. Phys. **66**, 129 (1994).
[57] G. Kotliar and J. Liu, Phys. Rev. B **38**, 5142 (1988).
[58] D. J. Scalapino, E. Loh, and J. E. Hirsch, Phys. Rev. B **34**, 8190 (1986).
[59] F. C. Zhang, C. Gros, T. M. Rice, and H. Shiba, Supercond. Sci. Technol. **1**, 36 (1988).
[60] D. S. Rokhsar, Phys. Rev. B **42**, 2526 (1990).
[61] Rokhsar's original theorem was proven for spin systems instead of fermion systems. But this theorem was formulated in the slave-fermion language, and the gauge constraint on the slave fermions becomes less and less important with increasing N. In the large-N limit, energetically, the slave fermions become physical fermions because the gauge field dynamics is completely suppressed in this limit.
[62] Y. Kohsaka, C. Taylor, K. Fujita, A. Schmidt, C. Lupien, T. Hanaguri, M. Azuma, M. Takano, H. Eisaki, H. Takagi *et al.*, Science **315**, 1380 (2007).
[63] S. Banerjee and E. Altman, Phys. Rev. B **95**, 134302 (2017).
[64] X. Chen, R. Fan, Y. Chen, H. Zhai, and P. Zhang, Phys. Rev. Lett. **119**, 207603 (2017).